

**MOLECULAR LEVEL ASPECTS OF BACTERIAL ADHESION,
TRANSPORT, AND BIOFILM FORMATION**

(Cosponsored with the Division of Colloid and Surface Chemistry
and the Division of Geochemistry)

Organized by

B.E. Logan, J. Kubicki and D. Velegol

Symposia Papers Presented Before the Division of Environmental Chemistry
American Chemical Society
New Orleans, LA March 23-27, 2003

**OBSERVATION, MEASUREMENT, AND MODELING OF BIOCOLLOID
DEPOSITION IN CROSSFLOW MEMBRANE FILTRATION**

Eric M.V. Hoek*, Seoktae Kang, and Marc A. Deshusses

Chemical and Environmental Engineering, University of California, Riverside, CA 91521

*Corresponding author, hoek@engr.ucr.edu

INTRODUCTION

Biofouling of membranes is one of the most severe of performance limiting problems that has deterred widespread application of membranes for water quality control¹. Biofouling may be defined as an unacceptable decline in performance due to the presence of a biofilm on a membrane surface². The initial stage of biofilm formation is controlled by deposition of microbes onto membrane surfaces. Deposition is governed by the transport of microorganisms (biocolloids) towards membrane surfaces and the interactions that govern biocolloid adhesion to membrane surfaces. Unlike simple colloids, microbes can exude extra-cellular polymeric substances (EPS) to facilitate adhesion³. Even when conditions are "unfavorable" for deposition, microbes may reside on or near the membrane surface (*i.e.*, in "secondary minima") under force of permeation drag long enough to exude these EPS and become strongly attached. The unique presence of a normal drag force aiding bio-adhesion presents a strikingly interesting system to study. Hence, the purpose of this investigation was to elucidate the fundamental mechanisms governing the deposition of biocolloids in crossflow membrane filtration.

While biofouling has historically limited reverse osmosis (RO) and nanofiltration (NF) processes, the current trend to pre-treat RO/NF feed waters by ultrafiltration (UF) has effectively transferred the biofouling problem to the UF membranes. In this study, the roles of permeation/crossflow velocities, solution/suspension characteristics, and membrane properties on biocolloid deposition were investigated through well-controlled

filtration experiments. Use of direct visual observation and individual particle tracking enabled quantification of net deposition rates. The physico-chemical characteristics of membranes and biocolloids were experimentally determined. The theoretical membrane-biocolloid DLVO interaction force was combined with transport forces such as permeation drag and inertial lift to shed valuable insight into the relative likelihood of deposition. Finally, the model estimates of biocolloid-membrane DLVO interaction forces were validated and refined by direct measurement using the atomic force microscope (AFM) colloid-probe technique⁴.

MATERIALS AND METHODS

Membranes, Model Biocolloids, and Reagents. In this study, two ultrafiltration membranes, MX50 and MX500 (Osmonics, Inc., Minnetonka, MN), were characterized by AFM and SEM for physical surface morphology and pore size properties according to the methods of⁵, as well as streaming potential for determination of membrane surface zeta potential by the methods of^{6,7}. In addition, the membrane performance properties (water permeability and solute retention) were systematically characterized via common filtration techniques.

Preliminary experiments utilized Fleishmann's active dry yeast cells (*Saccharomyces cerevisiae*). The model biocolloids were suspended in a buffer solution and stained with 4,6-Diamidino-2-phenylindole dihydrochloride (DAPI) to allow observation via fluorescence microscopy. Other experiments, not presented here, used 5.0 μm diameter fluorescent CML micro-spheres (Interfacial Dynamics, Oceanside, CA). Scanning electron microscopy (SEM) and potentiometric methods were used to verify microbe size and shape; electrophoretic mobility measurements were used to obtain biocolloid zeta potential as described in⁸.

All chemical solutions (stock electrolyte solutions, fluorescent dyes, and pH adjustors) were prepared using ACS or reagent grade chemicals from Fisher Scientific (Pittsburgh, PA) or Sigma-Aldrich (St. Louis, MO) dissolved in double distilled water that was deionized by a Milli-Q Synthesis Ultrapure water system (Millipore Corp.; Bedford, MA).

Direct Observation of Biofouling System. A novel crossflow membrane filter was designed and constructed in-house with a glass window over the crossflow chamber and mounted on a microscope stage to allow direct visual observation of microbial deposition via light and fluorescence microscopy. A 5 \times CCD camera was mounted on an Olympus microscope (Model BX 52), which provided 10, 40, or 100 \times magnification, and images were downloaded in real-time (up to 10 frames-per-second) to a computer equipped with image analysis software (OA/SIS). The flow channel dimensions are 1 mm high, 25 mm wide, and 76 mm long. A constant flow pump provides the feed flow rate and the combination of a bypass valve and back-pressure regulator allows fine control over the applied pressure and crossflow rate. The crossflow velocity is monitored by a rotameter and permeate velocity is kept constant by a peristaltic pump attached to the permeate line. Pressure transducers (Omega Model PX203; Stamford, CT) were installed at the feed, retentate, and permeate ports to determine the longitudinal and trans-membrane pressure drops in the system in a similar manner to

that employed by Ho and Zydney⁹. The setup described allows systematic variation of tangential (crossflow) and normal (permeate) velocities to aid in determining their role on adhesion of microorganisms to membrane surfaces.

Crossflow Membrane Filtration Experiments. At the beginning of each experiment, the system was equilibrated by filtering a particle free buffered electrolyte solution through the membrane to account for membrane compaction and other unknown causes of flux decline inherent to recirculating lab-scale filtration systems. Once performance stabilized, biocolloids were dosed directly into the feed tank to provide the desired feed biocolloid concentration.

RESULTS AND DISCUSSION

Model Biocolloid and Membrane Properties. Only results for MX50 and yeast cells are presented. Average yeast cell size was determined to be $4.89 \mu\text{m} \pm 1.88 \mu\text{m}$ via a Coulter Counter (Coulter Electronics, Ltd.; Beds, England). The zeta potential of yeast cells was determined to be approximately -15 mV at ionic strength of 10 mM NaCl and unadjusted pH of 5.7 from conversion of electrophoretic mobility measured by a ZetaPALS instrument (Brookhaven Instrument Corp., Brookhaven, NY). The pure water permeability of MX50 was determined to be $4.1 \times 10^{-10} \text{ m/Pa-s}$ (6.0 gfd/psi). The measured surface (zeta) potential was approximately -20 mV at ionic strength of 10 mM NaCl and unadjusted pH of 5.7. The UF membrane did not reject sodium chloride significantly, so the ionic strength at the membrane surface was considered equal to that in the bulk.

Since both membrane and model biocolloid surfaces were negatively charged it was hypothesized that at typical solution chemistries (pH 5.7 and 10 mM NaCl) conditions were generally unfavorable for deposition. To test this hypothesis, two experiments were conducted. All experimental conditions were constant between the two experiments except that in the first experiment there was no permeation through the membrane and in the second a moderate permeation velocity was applied. Note that even with no permeation, physical and chemical heterogeneities on the membrane and biocolloid surfaces were expected to produce some deposition.

Direct Observation of Biofouling (DOB) Experiments. In Figure 1, four images captured from experiments in the DOB system show the membrane surface during the electrolyte equilibration (*left*) and the membrane surface 60 minutes after yeast cells were dosed into the feed tank (*right*). Specific physico-chemical operating conditions included yeast cell concentration 50 mg/L (15.1×10^6 cells/mL), ionic strength 10 mM NaCl, unadjusted pH of 5.7, and cross flow velocities of 0.005 m/s ($Re = 10$). The principle difference between the two experiments depicted is that in the images at top there was no permeation through the membrane, whereas in the bottom images permeate flux was approximately $2.8 \times 10^{-5} \text{ m/s}$ (60 gfd). At left, dark areas are simply shadows due to misalignment of the light source, but bright patches are microbial deposits. Clearly more particles deposited on the membrane when a small permeation flux was applied; however, significant deposition is also seen for the experiment with no permeation. No significant flux decline (fouling) occurred for the short duration of these experiments.

Calculating Biocolloid-Membrane Interaction Forces. The rate of particle deposition in crossflow membrane filtration is governed by the transport of particles induced by convection, diffusion, and external forces¹⁰. In most aqueous environmental systems, the relevant external forces are colloidal and gravitational, where the colloidal force can be derived from the gradient of the total interaction potential¹⁰. Other short-range, non-DLVO interactions (*i.e.*, hydration, hydrophobic, steric, etc.) may be relevant for microbial deposition onto membranes, but inclusion of such forces is beyond the scope of this paper. Instead, a simple force balance is used to compare the “favorability” of the operating conditions on deposition for the experiments depicted in Fig. 1. The sphere-plate, constant surface potential interaction energy expression of Hogg et al.¹¹, which estimates the combined van der Waals and electrostatic interaction energy, was converted to a colloidal interaction force following¹². The total colloidal force is combined with the (attractive) gravitational force, the (attractive) Stokes drag force due to normal convection (permeation), and the (repulsive) inertial lift force¹³ due to tangential convection (cross flow) to provide semi-quantification of the likelihood of deposition occurring for each set of experimental conditions.

Figure 2 presents total interaction force plots for the experimental conditions used to obtain the images of Figure 1. In the case of $\sim 5 \mu\text{m}$ colloids, gravitational and inertial lift forces were negligible. It is clear that for both experiments there was a significant primary energy barrier. This verified that conditions were unfavorable for deposition in the primary minimum, but even without permeation the colloidal interactions produced a sizeable secondary minimum (see inset). The difference in the magnitude of total interaction force between the two curves is simply the effect of permeation drag (all other conditions were identical). From the force balance, it may be assumed that some yeast cells which deposited on the membrane (without permeation) resided in secondary minima. In fact, movies of biocolloid deposition captured in real-time during filtration showed that many yeast cells deposited and released, supporting the possibility of deposition in secondary minima.

Future Work. Other experimental work, not presented here, involved use of the AFM colloid-probe technique⁴ technique, in which $5 \mu\text{m}$ CML latex micro-spheres were affixed to a tip-less AFM cantilever allowing force-distance curves to be generated via. The total interaction force upon approach between the colloid-probe and membrane surface, as well as the pull-off adhesion force upon retraction were compared to the model predictions described above. The calculated and AFM measured interaction forces were in good qualitative agreement. In the future, AFM colloid-membrane force measurements will be used to refine the accuracy of colloidal force calculations to help better explain observed rates of microbial deposition. Moreover, it has been shown that inclusion of non-DLVO interaction forces may reduce or eliminate the primary energy barrier for deposition of various colloids onto polymeric reverse osmosis membranes¹⁴. Therefore, non-DLVO interactions may be incorporated into future analyses of colloidal forces.

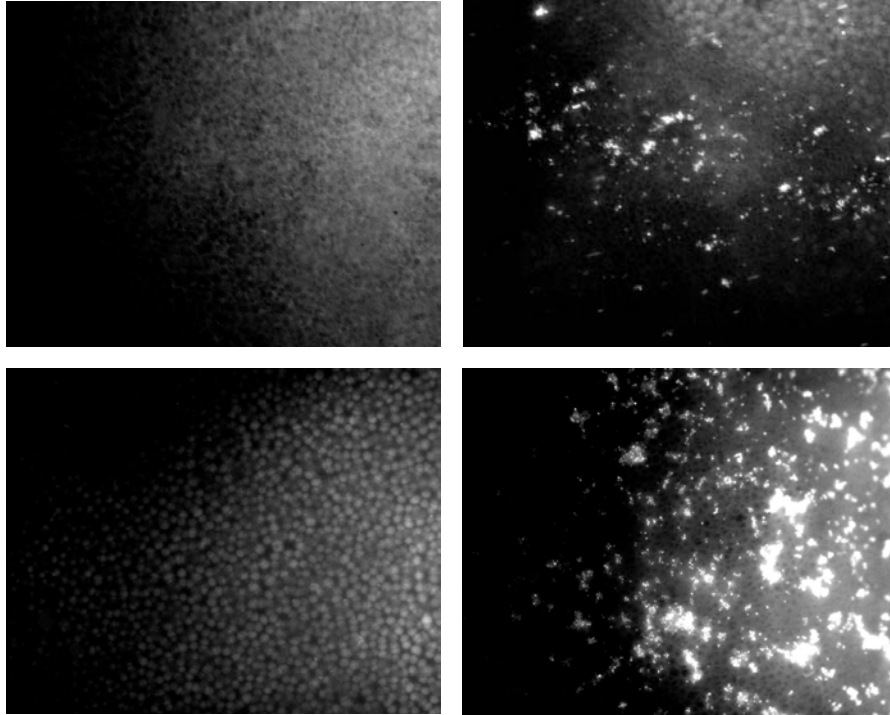


Figure 1: Microbial deposition (top) without and (bottom) with permeation through membrane. The images at left are prior to addition of Yeast cells to the feed tank and the images at right were taken 60 minutes after yeast cells were added.

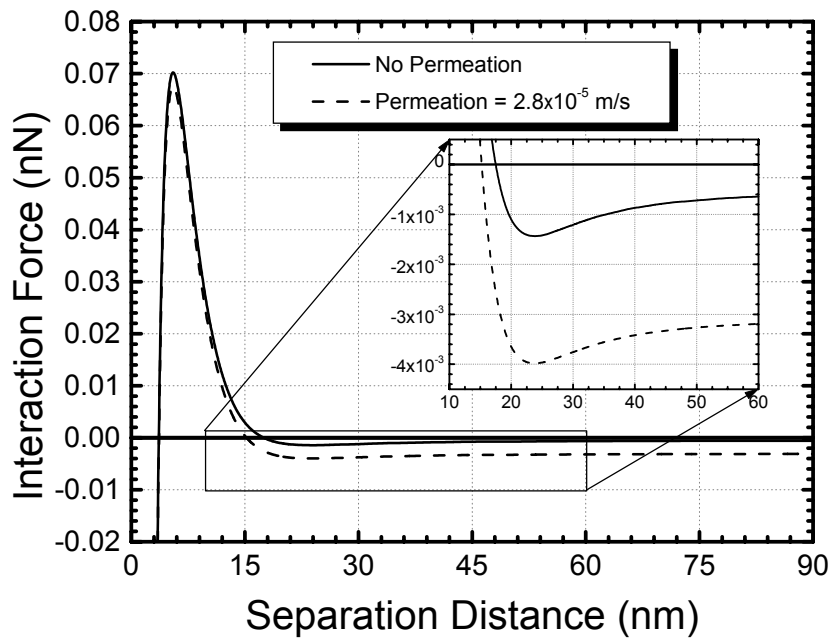


Figure 2: Total interaction force plots for DOB filtration experiments of Fig. 2 showing a secondary minimum predicted for the experiment involving permeation and no secondary minimum for the experiment without permeation.

REFERENCES

1. Ridgway, H., et al., *Biofouling of membranes: Membrane preparation, characterization, and analysis of bacterial adhesion*, in *Biofilms*. 1999. p. 463-494.
2. Flemming, H.C., et al., *Desalination*, 113 (1997) 215-225.
3. Characklis, W.G. and K.C. Marshall, *Biofilms*. Ecological and applied microbiology, ed. R. Mitchell. 1990, New York: John Wiley & Sons, Inc. 796.
4. Bowen, W.R., et al., *J. Colloid Interface Sci.*, 197 (1998) 348-352.
5. Fritzsche, A.K., et al., *J. Appl. Polym. Sci.*, 45 (1992) 1945-1956.
6. Walker, S.L., et al., 18 (2002) 2193-2198.
7. Childress, A.E. and M. Elimelech, *Journal of Membrane Science*, 119 (1996) 253-268.
8. VrijenHoek, E.M., et al., *J. Membr. Sci.*, 188 (2001) 115-128.
9. Ho, C.C. and A.L. Zydney, 209 (2002) 363-377.
10. Song, L.F. and M. Elimelech, *J. Colloid Interface Sci.*, 173 (1995) 165-180.
11. Hogg, R.I., et al., *Trans. Faraday Soc.*, 62 (1966) 1638-1651.
12. Tobiason, J.E., *Physicochemical aspects of particle deposition in porous media*, in *Geography and Environmental Engineering*. 1987, The Johns Hopkins University: Baltimore, MD. p. 296.
13. Williams, P.S., et al., *Colloid Surf. A*, 113 (1996) 215-228.
14. Brant, J.A. and A.E. Childress, *J. Membr. Sci.*, 203 (2002) 257-273.